

**SYNTHESIS, STRUCTURE AND PROPERTIES OF A HETEROMETALLIC 4f-5d COMPLEX [Sm(Hinic)<sub>3</sub>(H<sub>2</sub>O)<sub>2</sub>]<sub>n</sub>·(1.5nHgCl<sub>4</sub>)·(2nH<sub>2</sub>O)**

Wentong CHEN

School of Chemistry and Chemical Engineering,  
Jiangxi Province Key Laboratory of Coordination Chemistry, Jinggangshan University,  
Ji'an, Jiangxi 343009, China; e-mail: wtchen\_2000@yahoo.cn

Received May 24, 2010

Accepted February 2, 2011

Published online March 2, 2011

A novel complex with samarium and mercury [Sm(Hinic)<sub>3</sub>(H<sub>2</sub>O)<sub>2</sub>]<sub>n</sub>·(1.5nHgCl<sub>4</sub>)·(2nH<sub>2</sub>O) (**1**) (Hinic = pyridine-4-carboxylic acid, i.e. isonicotinic acid), has been synthesized via hydrothermal reaction and structurally characterized. Complex **1** is characteristic of a one-dimensional polycationic chain-like structure. Photoluminescent investigation reveals that the title complex displays interesting emissions in violet, blue, green, orange and red regions. The luminescence spectra show the stronger violet and blue emissions than the green, orange and red ones. The green, orange and red emission bands are attributed to the characteristic emissions of <sup>4</sup>G<sub>5/2</sub>→<sup>6</sup>H<sub>J</sub> (J = 5/2, 7/2, 9/2) of Sm<sup>3+</sup> ions. Optical absorption spectra of **1** reveal the presence of a wide optical bandgap of 3.27 eV. The magnetic properties show that complex **1** exhibits antiferromagnetic-like interactions.

**Keywords:** Crystal structure; Hydrothermal; Hybrid; Photoluminescence; Antiferromagnetic.

Currently, the increasing interest in the field of the crystal engineering of inorganic-organic hybrid materials is justified by the potential applications of these materials as catalysis, magnetic functional materials, zeolite-like materials, biology, and so forth<sup>1-4</sup>. Besides, there is also an aesthetic perspective: for the vast amount of inorganic-organic hybrid materials, the intriguing variety of the architectures and topologies that can be obtained by self-assembling metal ions and multifunctional ligands attract chemists. In recent years, the synthesis of inorganic-organic hybrid materials based on transition metals has become widespread<sup>5-9</sup>. Similarly, a wealth of reports on lanthanide-based inorganic-organic hybrid materials have been reported thus far<sup>10-13</sup>. To our knowledge, lanthanide-based inorganic-organic hybrid materials with aromatic carboxylic acids exhibit good thermal and luminescent stability for practical application.

Inic<sup>-</sup> is a quite interesting tecton in constructing extended structures because it is an unsymmetrical divergent ligand with a nitrogen atom at one

end and two oxygen atoms from the carboxylato group at the other one.  $\text{Inic}^-$  can link two metal centers by coordinating to a metal center with the nitrogen atom and, to the other one, with one or two carboxylato oxygen atoms<sup>14,15</sup>. Therefore,  $\text{inic}^-$  has been used to prepare novel compounds and a number of isonicotinate lanthanide compounds have so far been reported, because they are potentially useful materials in the areas like luminescence<sup>16–20</sup>, magnet<sup>21–28</sup> metallacrowns<sup>29</sup>, and so forth. To our knowledge, among the isonicotinate lanthanide compounds, less are transition metal containing. Actually, LN-TM-based (LN = lanthanide, TM = transition metal) inorganic-organic hybrid materials with aromatic carboxylic acids as ligands may have novel structural topologies and properties, such as luminescence<sup>30–33</sup> and magnetism<sup>34–40</sup>. Consequently, LN-TM- $\text{inic}^-$  compounds have yet to be explored.

Therefore, we became interested in the crystal engineering of LN-TM-based inorganic-organic hybrid materials with  $\text{Hinic}^-$  as ligand. We herein report the synthesis, structure and properties of  $[\text{Sm}(\text{Hinic})_3(\text{H}_2\text{O})_2]_n \cdot (1.5n\text{HgCl}_4) \cdot (2n\text{H}_2\text{O})$  (**1**).

## EXPERIMENTAL

### Materials and Instrumentation

All reactants, A. R. grade quality, were obtained commercially and used without further purification. Elemental analyses of carbon, hydrogen and nitrogen were carried out with an Elementar Vario EL (Elementar Analysen System GmbH, Germany). Infrared Spectra were obtained with a Perkin–Elmer spectrum one FT-IR spectrometer using KBr discs. The fluorescent data were collected at room temperature on a computer-controlled Jobin Yvon FluoroMax-3 spectrometer (France) in fluorescence mode. The UV-Vis spectra were recorded at room temperature on a computer-controlled Perkin–Elmer Lambda 35 UV/Vis spectrometer equipped with an integrating sphere in the wavelength range 190–2500 nm.  $\text{BaSO}_4$  plate was used as a reference (100% reflectance), on which the finely ground powders of the samples were coated. The absorption spectra were calculated from reflection spectra by the Kubelka–Munk function:  $\alpha/S = (1 - R)^2/2R$ , where  $\alpha$  is the absorption coefficient,  $S$  is the scattering coefficient which is practically wavelength independent when the particle size is larger than 5  $\mu\text{m}$ , and  $R$  is the reflectance. The energy band gaps were determined by extrapolation from the linear portion of the absorption edge in an  $\alpha/S$  versus energy plot from the UV-Vis diffuse spectra<sup>41,42</sup>. Variable-temperature magnetic susceptibility measurement of the title complex on polycrystalline samples was performed on a PPMS 9T Quantum Design SQUID magnetometer (USA). All data were corrected for diamagnetism estimated from Pascal's constants. Semiquantitative microscope analysis was performed on a field emission scanning electron microscope (Hitachi FESEM, JEOL JSM6700F) equipped with an energy dispersive X-ray spectroscopy (EDS).

Synthesis of  $[\text{Sm}(\text{Hinic})_3(\text{H}_2\text{O})_2]_n \cdot (1.5n\text{HgCl}_4) \cdot (2n\text{H}_2\text{O})$  (**1**)

The title complex was prepared by mixing  $\text{SmCl}_3 \cdot 6\text{H}_2\text{O}$  (1 mmol, 365 mg),  $\text{HgCl}_2$  (1.5 mmol, 408 mg), Hinic (3 mmol, 369 mg) and distilled water (10 ml) in a 25-ml Teflon-lined stainless steel autoclave and heated at 200 °C for 10 days. After being slowly cooled to room temperature at 6 °C/h, colorless crystals suitable for X-ray analysis were obtained. The yield was 62% (based on mercury). Analysis of the product with SEM/EDS showed the presence of Sm, Hg and Cl in a ratio of 1:1.49:5.92, which is close to the chemical formula of  $\text{SmHg}_{1.5}\text{Cl}_6$  established by the X-ray diffraction analysis. For  $\text{C}_{36}\text{H}_{46}\text{Cl}_{12}\text{Hg}_3\text{N}_6\text{O}_{20}\text{Sm}_2$  calculated: 19.54% C, 2.08% H, 3.80% N; found: 19.38% C, 2.05% H, 3.71% N. IR (KBr,  $\text{cm}^{-1}$ ): 3421 (vs), 1690 (m), 1591 (vs), 1412 (vs), 1225 (m), 1077 (w), 1048 (w), 844 (s), 761 (vs), 680 (s), 537 (m), 416 (m).

## X-ray Structure Determination

The intensity data set was collected on a Rigaku Mercury CCD X-ray diffractometer with graphite monochromated  $\text{MoK}\alpha$  radiation ( $\lambda = 0.71073 \text{ \AA}$ ) using a  $\omega$  scan technique. CrystalClear software was used for data reduction and empirical absorption corrections<sup>43</sup>. The structure was solved by the direct method using the Siemens SHELXTL™ Version 5 package of crystallographic software<sup>44</sup>. The difference Fourier maps based on these atomic positions yield the other non-hydrogen atoms. The hydrogen atom positions were generated theoretically, except for those on the lattice water molecules these are yielded by the difference Fourier maps, allowed to ride on their respective parent atoms and included in the structure factor calculations with assigned isotropic thermal parameters but were not refined. The structures were refined using a full-matrix least-squares refinement on  $F^2$ . All atoms were refined anisotropically. The positive/negative residual densities are 2.550/−3.074  $\text{e}/\text{\AA}^3$  (0.91  $\text{\AA}$  from Cl2 and 0.90  $\text{\AA}$  from Sm1, respectively), which are resulted from the heavy atoms like samarium. A summary of crystallographic data and structure analysis is listed in Table I, selected bond distances and bond angles are given in Table II. CCDC 654683 contains the supplementary crystallographic data for this paper. These data can be obtained free of charge via [www.ccdc.cam.ac.uk/conts/retrieving.html](http://www.ccdc.cam.ac.uk/conts/retrieving.html) (or from the Cambridge Crystallographic Data Centre, 12, Union Road, Cambridge, CB2 1EZ, UK; fax: +44 1223 336033; or [deposit@ccdc.cam.ac.uk](mailto:deposit@ccdc.cam.ac.uk)).

## RESULTS AND DISCUSSION

The intense vibration of 3421  $\text{cm}^{-1}$  is assigned to the characteristic peak of OH vibration of water molecules. The strong vibrations locating at 1591 and 1412  $\text{cm}^{-1}$  correspond to the asymmetric and symmetric stretching vibrations of the carboxylate group of the Hinic ligands, respectively. The existence of the band at 1690  $\text{cm}^{-1}$  indicates the Hinic are protonated<sup>45</sup>.

The structure of **1** consists of  $[\text{Sm}(\text{Hinic})_3(\text{H}_2\text{O})_2]_n^{3n+}$  cationic moieties,  $\text{HgCl}_4^{2-}$  anions and isolated water molecules, as shown in Fig. 1. The Hg1 atom is tetrahedrally bound by four chlorine atoms to form a  $\text{HgCl}_4^{2-}$  anion with the bond lengths of Hg–Cl ranging from 2.434(2) to 2.581(1)  $\text{\AA}$  with an average value of 2.488(1)  $\text{\AA}$ , which are comparable with the counterparts

found in literature<sup>46,47</sup>. The Hg2 atom is positional disordered and the occupancy of Hg2 must be set to 0.5 to get rational structure model and thermal displacement parameters. The samarium atom is coordinated by eight oxygen atoms, of which two are from two water molecules and six from six Hinic ligands, yielding a distorted square antiprism with the top and bottom planes defined by O(3), O(4W), O(5), O(6) ( $1 - x, y, 5/2 - z$ ) and O(1), O(3W), O(4) ( $1/2 - x, 1/2 - y, 2 - z$ ), O(2) ( $1 - x, y, 5/2 - z$ ) atoms, respectively. The bond lengths of Sm–O<sub>Hinic</sub> range from 2.365(3) to 2.425(3) Å with an average value of 2.394(2) Å, which is obviously shorter than that of Sm–O<sub>water</sub> being of 2.503(3) and 2.538(2) Å, indicating that Hinic ligand

TABLE I  
Summary of crystallographic data and structure analysis of 1

Formula	C <sub>36</sub> H <sub>46</sub> Cl <sub>12</sub> Hg <sub>3</sub> N <sub>6</sub> O <sub>20</sub> Sm <sub>2</sub>
Formula weight	2210.66
Color	colorless
Crystal size, mm <sup>3</sup>	0.20 × 0.06 × 0.05
Crystal system	monoclinic
Space group	C2/c
<i>a</i> , Å	24.288(8)
<i>b</i> , Å	20.895(2)
<i>c</i> , Å	15.376(8)
β, °	127.919(9)
<i>V</i> , Å <sup>3</sup>	6156(4)
<i>Z</i>	4
2θ <sub>max</sub> , °	54.96
Reflections collected	23567
Independent, observed reflections ( <i>R</i> <sub>int</sub> )	7011, 2872 (0.1158)
<i>D</i> <sub>calc</sub> , g/cm <sup>3</sup>	2.385
μ, mm <sup>-1</sup>	9.926
<i>T</i> , K	293(2)
<i>F</i> (000)	4128
<i>R</i> 1, <i>wR</i> 2	0.0625, 0.1105
<i>S</i>	0.956
Largest and mean Δ/σ	0.001, 0
Δρ (max/min), e/Å <sup>3</sup>	2.550/−3.074

has a stronger affinity to Sm(III) ion than that of water. The coordination polyhedron of the samarium ion in **1** is similar to that reported before<sup>48–50</sup>. All the three crystallographic independent Hinc ligands act as bidentate ligands to bridge two neighboring samarium atoms and the nitrogen atoms of the Hinc ligands should be protonated, as the case found in many other references<sup>51,52</sup>. The samarium atoms are alternately bridged by two or four  $\mu_2$ -Hinc ligands in a  $(-2-4)_n$  (the number indicates the number of the bridges) mode to construct a 1D cationic chain with the Sm...Sm distances of ca. 5.042 and 4.589 Å, respectively. The 1D cationic chains,  $\text{HgCl}_4^{2-}$  moieties and water molecules are linked by electrostatic interactions and hydrogen bonds to yield a 3D supramolecular network (Fig. 2).

Taking into account the excellent luminescent property of  $\text{Sm}^{3+}$  ion, the solid-state luminescence of **1** was investigated at room temperature (Fig. 3). The solid-state excitation spectra of the title complex show that the effec-

TABLE II  
Selected bond lengths and angles

Bond length	Å	Bond angle	°
Hg1–Cl1	2.469(1)	Cl2–Hg1–Cl3	117.31(5)
Hg1–Cl2	2.434(2)	Cl2–Hg1–Cl1	113.83(5)
Hg1–Cl3	2.468(2)	Cl3–Hg1–Cl1	109.61(6)
Hg1–Cl4	2.581(1)	Cl2–Hg1–Cl4	104.06(5)
Hg2–Cl5	2.458(3)	Cl3–Hg1–Cl4	104.71(5)
Hg2–Cl6	2.266(2)	Cl1–Hg1–Cl4	106.12(4)
Hg2–Cl6#1	2.618(2)	Cl6–Hg2–Cl7	109.64(8)
Hg2–Cl7	2.432(3)	Cl6–Hg2–Cl5	122.59(5)
Hg2–Cl7#1	2.432(3)	Cl7–Hg2–Cl5	90.75(7)
Sm1–O1	2.393(3)	Cl6–Hg2–Cl6#1	111.28(7)
Sm1–O2#2	2.425(3)	Cl7–Hg2–Cl6#1	111.29(7)
Sm1–O3	2.390(3)	Cl5–Hg2–Cl6#1	109.44(5)
Sm1–O4#3	2.388(3)		
Sm1–O5	2.400(3)		
Sm1–O6#2	2.365(3)		
Sm1–O3W	2.503(3)		
Sm1–O4W	2.538(2)		

Symmetry codes: #1  $-x + 1, y, -z + 7/2$ ; #2  $-x + 1, y, -z + 5/2$ ; #3  $-x + 1/2, -y + 1/2, -z + 2$ .

tive energy absorption mainly takes place in the long wavelength ultraviolet region of the range of 280–390 nm. The excitation band of complex **1** under the emission of 413 nm possesses one main peak of 329 nm. We further measured the corresponding emission spectra using the excitation wavelength of 329 nm for the title complex, and we obtained the emission spectra (shown in Fig 3). For complex **1**, the emission spectra shows three emission bands under the excitation of 329 nm: 562, 598 and 643 nm, corresponded to the characteristic emission  ${}^4G_{5/2} \rightarrow {}^6H_J$  ( $J = 5/2, 7/2, 9/2$ ) of  $\text{Sm}^{3+}$  ions<sup>53–55</sup>. Among the three characteristic emissions  ${}^4G_{5/2} \rightarrow {}^6H_J$  ( $J = 5/2, 7/2, 9/2$ ) of  $\text{Sm}^{3+}$  ions, the orange emission intensity of  ${}^4G_{5/2} \rightarrow {}^6H_{7/2}$  transition is stronger than the green and red emissions of  ${}^4G_{5/2} \rightarrow {}^6H_{5/2}$  and  ${}^4G_{5/2} \rightarrow {}^6H_{9/2}$ . Except for these three emission bands, upon the photoexcitation of 329 nm, there are other intense bands with the maximum wavelength located at 396, 413, 426 and 495 nm, respectively, all are stronger than the three characteristic emissions  ${}^4G_{5/2} \rightarrow {}^6H_J$  ( $J = 5/2, 7/2, 9/2$ ) of  $\text{Sm}^{3+}$  ions. These intense emission bands can probably arise from ligand luminescence.

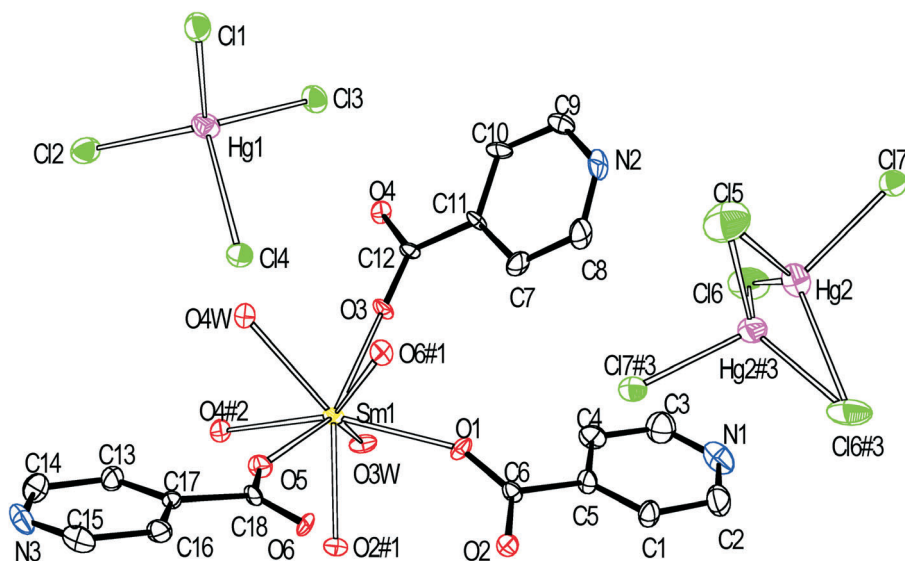


FIG. 1

ORTEP drawing of **1** with 30% thermal ellipsoids. Lattice water molecules and hydrogen atoms are omitted for clarity. Symmetry codes – #1:  $1 - x, y, 5/2 - z$ ; #2:  $1/2 - x, 1/2 - y, 2 - z$ ; #3:  $1 - x, y, 7/2 - z$

Optical absorption spectrum of **1** reveals the presence of an obvious optical bandgap of 3.27 eV (Fig. 4), which suggests that complex **1** may be a potential wide-gap semiconductor. The gradual slope of the optical absorption edge for **1** is indicative of the existence of indirect transitions<sup>56</sup>. Samarium ions contribute the small absorption peaks in ca. 1252, 1097, 946, 473 and 400 nm. These are evidently f–f transitions from Sm(III), from  $^6H_{5/2}$  to the  $^6F$  manifold (energies between 6400 and 10500  $\text{cm}^{-1}$  approximately) and, possibly internal transitions to the  $^6H$  manifolds (energies between 1000 and 6600  $\text{cm}^{-1}$  approximately).

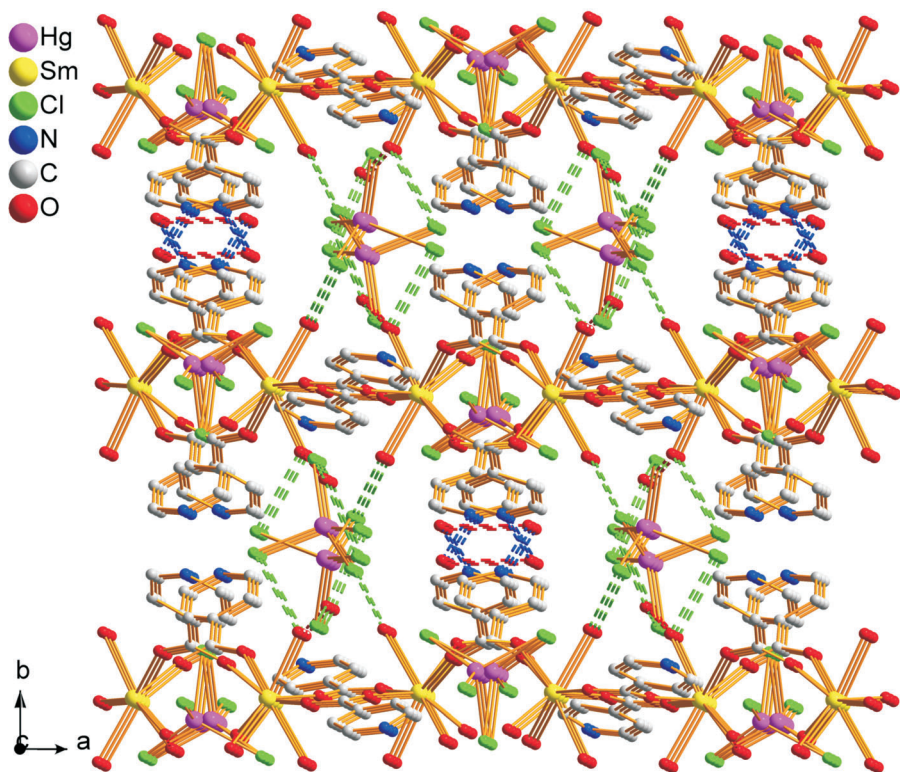


FIG. 2

Packing diagram of **1** with the dashed lines representing hydrogen bonds (in Å): O2W...N1 ( $x, 1 - y, -0.5 + z$ ) 2.867(5), O2W...O2W ( $1 - x, y, 2.5 - z$ ) 3.015(4), O1W...O4W 2.759(4), O1W...Cl1 ( $x, -y, -0.5 + z$ ) 3.175(4), O1W...Cl2 3.246(3), O3W...Cl3 ( $0.5 - x, 0.5 - y, 2 - z$ ) 3.199(3) and O4W...Cl4 3.199(3)

The magnetic susceptibility of **1** was investigated from 300 to 2 K at 5000 Oe on the polycrystalline samples (Fig. 5). When decreasing the temperature, the  $x_M T$  of **1** decreases gradually from 0.29 cm<sup>3</sup> K/mol at 300 K to reach 0.05 cm<sup>3</sup> K/mol at 2 K. This behavior is typically observed for paramagnetic systems that exhibit dominating antiferromagnetic-like interactions. The curve fit for  $x_M$  vs  $T$  plot of **1** with the Curie–Weiss law in the whole range

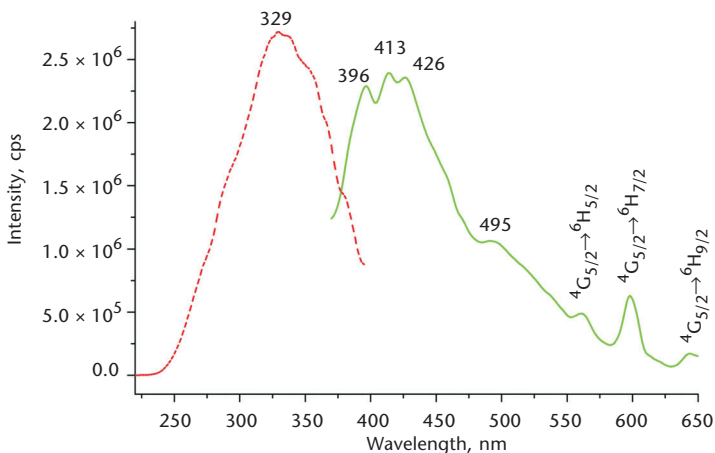


FIG. 3  
Solid-state emission (solid line) and excitation (dashed line) spectra of **1**

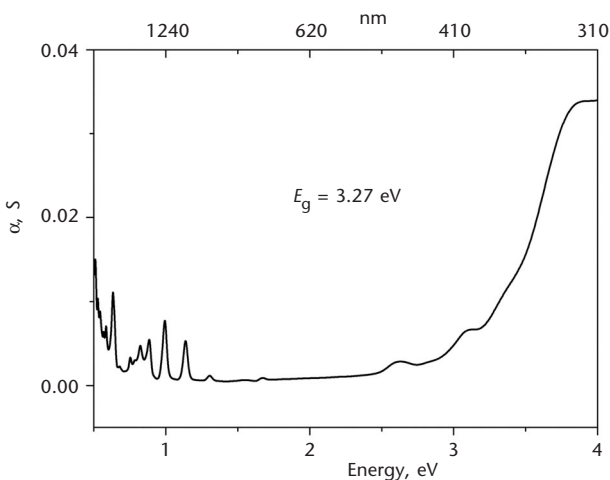


FIG. 4  
Solid-state diffuse reflectance spectrum of **1**

of 2–300 K give good result with  $C = 0.26 \text{ cm}^3 \text{ K/mol}$  and  $\theta = -0.41 \text{ K}$  for **1**. The small negative Weiss constant suggests weak antiferromagnetic-like interactions between the  $\text{Sm}^{3+}$  ions. Further analysis of the magnetic data will be carried out later when suitable model is found to fit the data. The field dependence of the magnetization for **1** measured at 2 K reveals a hysteresis loop with a coercive field of ca. 11 Oe and remnant magnetization of  $4.5 \times 10^{-5} N\beta$ , suggesting the paramagnetic behavior of **1** (Fig. 6). The magnetiza-

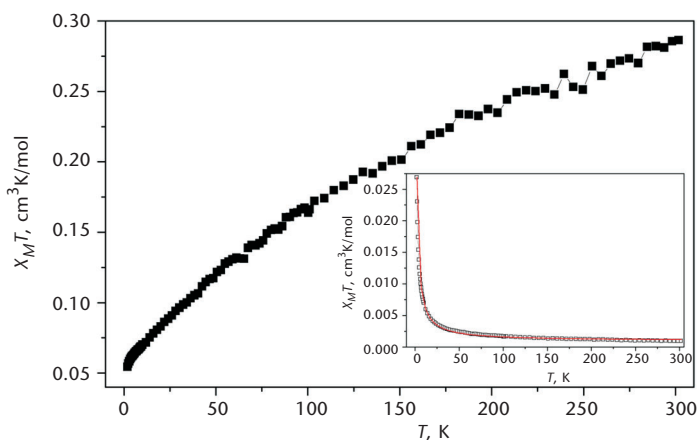


FIG. 5

A graph of  $\chi_M T$  vs  $T$  of **1**. Inset:  $\chi_M T$  vs  $T$  of **1** (the red full line corresponds to the best data fit)

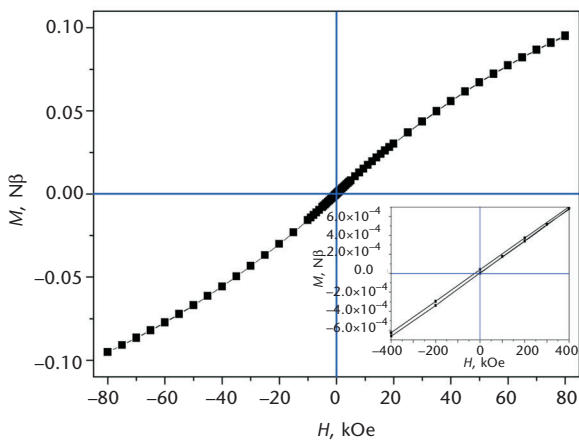


FIG. 6

Magnetization vs  $H$  at 2 K for **1**. Inset: Expansion showing the small coercivity

tion increases fast with increasing field first, and then slowly. Clearly, the saturation of magnetization for **1** is still not reached up to 80 kOe with a value of  $0.10 N\beta$ .

## CONCLUSION

In brief, a new complex with samarium and mercury via hydrothermal reaction was successfully prepared. The title complex shows interesting emissions in a broad region. The emission bands are attributed to the characteristic emissions of  ${}^4G_{5/2} \rightarrow {}^6H_J$  ( $J = 5/2, 7/2, 9/2$ ) of  $\text{Sm}^{3+}$  ions. Optical absorption spectra show that the title complex may be a candidate for potential photoelectric material. Magnetic measurements indicate that the title complex exhibits antiferromagnetic-like interactions.

*The author gratefully acknowledges the financial support of the NSF of Jiangxi Province (200007GQH1685 and 2008GQH0001).*

## REFERENCES

1. Fujita M., Kwon Y. J., Washizu S., Ogura K.: *J. Am. Chem. Soc.* **1994**, *116*, 1151.
2. Dunbar K. M., Heintz R. A.: *Prog. Inorg. Chem.* **1997**, *45*, 283.
3. Kepert C. J., Rosseinsky M. J.: *Chem. Commun.* **1999**, 375.
4. Eddaoudi M., Moler D. B., Li H., Chen B., Reinecke T. M., O'Keeffe M., Yaghi O. M.: *Acc. Chem. Res.* **2001**, *34*, 319.
5. Janiak C.: *Angew. Chem., Int. Ed. Engl.* **1997**, *36*, 1431.
6. Yaghi O. M., Li H., Davis C., Richardson D., Groy T. L.: *Acc. Chem. Res.* **1998**, *31*, 474.
7. Batten S. R., Robson R.: *Angew. Chem., Int. Ed. Engl.* **1998**, *37*, 1460.
8. Lin W., Evans O. R., Xiong R. G., Wang Z.: *J. Am. Chem. Soc.* **1998**, *120*, 13272.
9. Evans O. R., Xiong R. G., Wang Z., Wong G. K., Lin W.: *Angew. Chem., Int. Ed.* **1999**, *38*, 536.
10. Reinecke T. M., Eddaoudi M., Fehr M., Kelley D., Yaghi O. M.: *J. Am. Chem. Soc.* **1999**, *121*, 1651.
11. Andruh M., Costes J. P., Diaz C., Gao S.: *Inorg. Chem.* **2009**, *48*, 3342.
12. Binnemans K.: *Chem. Rev.* **2009**, *109*, 4283.
13. Eliseeva S. V., Bünzli J.-C. G.: *Chem. Soc. Rev.* **2010**, *39*, 189.
14. Lu J. Y., Babb A. M.: *Chem. Commun.* **2001**, 821.
15. Chapman M. E., Ayyappan P., Foxman B. M., Yee G. T., Lin W.: *Cryst. Growth Des.* **2001**, *1*, 159.
16. Jia G., Law G.-L., Wong K.-L., Tanner P. A., Wong W.-T.: *Inorg. Chem.* **2008**, *47*, 9431.
17. Ma L., Evans O. R., Foxman B. M., Lin W.: *Inorg. Chem.* **1999**, *38*, 5837.
18. Wang C.-M., Wu Y.-Y., Chang Y.-W., Lii K.-H.: *Chem. Mater.* **2008**, *20*, 2857.
19. Binnemans K.: *Chem. Rev.* **2009**, *109*, 4283.
20. Horrocks W. DeW., Jr., Sudnick D. R.: *J. Am. Chem. Soc.* **1979**, *101*, 334.
21. Gao Y., Xu G.-F., Zhao L., Tang J., Liu Z.: *Inorg. Chem.* **2009**, *48*, 11495.

22. Liu F.-C., Zeng Y.-F., Jiao J., Li J.-R., Bu X.-H., Ribas J., Batten S. R.: *Inorg. Chem.* **2006**, *45*, 6129.
23. Bünzli J.-C. G., Piquet C.: *Chem. Rev.* **2002**, *102*, 1897.
24. Ke H., Gamez P., Zhao L., Xu G.-F., Xue S., Tang J.: *Inorg. Chem.* **2010**, *49*, 7549.
25. Hu X., Zeng Y.-F., Chen Z., Sanudo E. C., Liu F.-C., Ribas J., Bu X.-H.: *Cryst. Growth Des.* **2009**, *9*, 421.
26. Xu J., Su W., Hong M.: *Cryst. Growth Des.* **2011**, *11*, 337.
27. Yang Y.-F., Ma Y.-S., Guo L.-R., Zheng L.-M.: *Cryst. Growth Des.* **2008**, *8*, 1213.
28. Baggio R., Calvo R., Garland M. T., Peña O., Percec M., Rizzi A.: *Inorg. Chem.* **2005**, *44*, 8979.
29. Mezei G., Zaleski C. M., Pecoraro V. L.: *Chem. Rev.* **2007**, *107*, 4933.
30. Sun H.-Y., Huang C.-H., Jin X.-L., Xu G.-X.: *Polyhedron* **1995**, *14*, 1201.
31. Song J.-L., Yi F.-Y., Mao J.-G.: *Cryst. Growth Des.* **2009**, *9*, 3273.
32. Zhou R.-S., Cui X.-B., Song J.-F., Xu X.-Y., Xu J.-Q., Wang T.-G.: *J. Solid State Chem.* **2008**, *181*, 2099.
33. Bai Y.-Y., Huang Y., Yan B., Song Y.-S., Weng L.-H.: *Inorg. Chem. Commun.* **2008**, *11*, 1030.
34. Andruh M., Ramade I., Codjovi E., Guillou O., Kahn O., Trombe J. C.: *J. Am. Chem. Soc.* **1993**, *115*, 1822.
35. Novitchi G., Wernsdorfer W., Chibotaru L. F., Costes J.-P., Anson C. E., Powell A. K.: *Angew. Chem., Int. Ed.* **2009**, *48*, 1614.
36. Kido T., Ikuta Y., Sunatsuki Y., Ogawa Y., Matsumoto N., Re N.: *Inorg. Chem.* **2003**, *42*, 398.
37. Costes J.-P., Auchel M., Dahan F., Peyrou V., Shova S., Wernsdorfer W.: *Inorg. Chem.* **2006**, *45*, 1924.
38. Mishra A., Tasiopoulos A. J., Wernsdorfer W., Abboud K. A., Christou G.: *Inorg. Chem.* **2007**, *46*, 3105.
39. Zaleski C. M., Kampf J. W., Mallah T., Kirk M. L., Pecoraro V. L.: *Inorg. Chem.* **2007**, *46*, 1954.
40. Andruh M., Ramade I., Codjovi E., Guillou O., Kahn O., Trombe J. C.: *J. Am. Chem. Soc.* **1993**, *115*, 1822.
41. Wendlandt W. W., Hecht H. G.: *Reflectance Spectroscopy*. Interscience Publishers, New York 1966.
42. Kortüm G.: *Reflectance Spectroscopy*. Springer Verlag, New York 1969.
43. *CrystalClear*, Version 1.35. Rigaku Corp., Tokyo 2002.
44. *SHELXTL*, Version 5, Reference Manual. Siemens Energy & Automation Inc., Madison (WI) 1994.
45. Zhong Z.-E., Sun D.-F.: *Chin. J. Struct. Chem.* **2001**, *20*, 478.
46. Schoberl U., Magnera T. F., Harrison R. M., Fleischer F., Pflug J. L., Schwab P. F. H., Meng X., Lipiak D., Noll B. C., Allured V. S., Rudalevige T., Lee S., Michl J.: *J. Am. Chem. Soc.* **1997**, *119*, 3907.
47. Chen W. T., Wang M. S., Liu X., Guo G. C., Huang J. S.: *Cryst. Growth Des.* **2006**, *6*, 2289.
48. Wu K.-J., Cai L.-Z., Xu G., Zhou G.-W., Guo G.-C.: *Acta Crystallogr. E* **2008**, *64*, m56.
49. Yan B., Xie Q. Y.: *J. Mol. Struct.* **2004**, *688*, 73.
50. Xu J., Han J.-J., Zheng S.-T., Yang G.-Y.: *Chin. J. Struct. Chem.* **2006**, *25*, 866.

51. Cotton F. A., Falvello L. R., Reid A. H., Roth W. J.: *Acta Crystallogr., Sect. C: Cryst. Struct. Commun.* **1990**, *46*, 1815.
52. Chen S. M., Lu C. Z., Yu Y. Q., Zhang Q. Z., He X.: *Acta Crystallogr., Sect. C: Cryst. Struct. Commun.* **2004**, *60*, m437.
53. Huang Y. G., Yuan D. Q., Gong Y. Q., Jiang F. L., Hong M. C.: *J. Mol. Struct.* **2008**, *872*, 99.
54. Song Y. S., Yan B., Chen Z. X.: *J. Solid State Chem.* **2004**, *177*, 3805.
55. Yan B., Zhou B., Wang Q. M.: *Appl. Organometal. Chem.* **2006**, *20*, 835.
56. Huang F. Q., Mitchell K., Ibers J. A.: *Inorg. Chem.* **2001**, *40*, 5123.